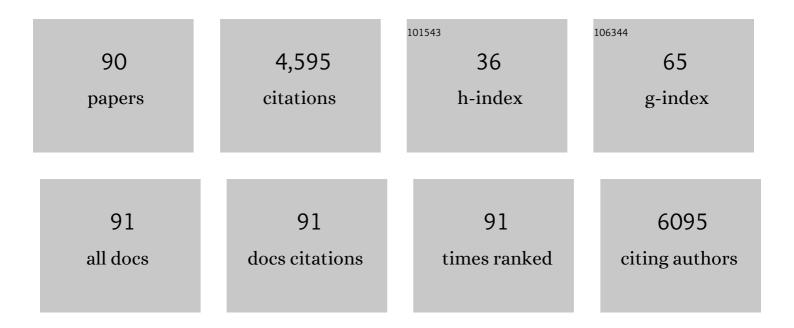
## **Tian Sheng**

List of Publications by Year in descending order

Source: https://exaly.com/author-pdf/340365/publications.pdf Version: 2024-02-01



TIAN SHENC

#	Article	IF	CITATIONS
1	Regulating the nanoscale intimacy of metal and acidic sites in Ru/γ-Al2O3 for the selective conversions of lignin-derived phenols to jet fuels. Journal of Energy Chemistry, 2022, 66, 576-586.	12.9	35
2	High activity of step sites on Pd nanocatalysts in electrocatalytic dechlorination. Physical Chemistry Chemical Physics, 2022, 24, 3896-3904.	2.8	10
3	Boosting Electrocatalytic Hydrazine Oxidation Reaction on High-Index Faceted Au Concave Trioctahedral Nanocrystals. ACS Sustainable Chemistry and Engineering, 2022, 10, 696-702.	6.7	11
4	Outstanding long-cycling lithiumâ^'sulfur batteries by core-shell structure of S@Pt composite with ultrahigh sulfur content. , 2022, 1, 100006.		45
5	High CO-Tolerant Ru-Based Catalysts by Constructing an Oxide Blocking Layer. Journal of the American Chemical Society, 2022, 144, 9292-9301.	13.7	29
6	Electrocatalysis CO <sub>2</sub> to Tunable Syngas upon Fe Clusters Catalyst Dispersed on Bamboo-like NCTs. Inorganic Chemistry, 2022, 61, 9375-9380.	4.0	6
7	Li-CO2/O2 battery operating at ultra-low overpotential and low O2 content on Pt/CNT catalyst. Chemical Engineering Journal, 2022, 448, 137541.	12.7	18
8	Structurally Disordered Phosphorus-Doped Pt as a Highly Active Electrocatalyst for an Oxygen Reduction Reaction. ACS Catalysis, 2021, 11, 355-363.	11.2	79
9	Iron Doped in the Subsurface of CuS Nanosheets by Interionic Redox: Highly Efficient Electrocatalysts toward the Oxygen Evolution Reaction. ACS Applied Materials & Interfaces, 2021, 13, 16210-16217.	8.0	31
10	Ultrasmall Pt Nanoparticles-Loaded Crystalline MoO <sub>2</sub> /Amorphous Ni(OH) <sub>2</sub> Hybrid Nanofilms with Enhanced Water Dissociation and Sufficient Hydrogen Spillover for Hydrogen Generation. ACS Sustainable Chemistry and Engineering, 2021, 9, 8257-8269.	6.7	18
11	Singlet oxygen triggered by robust bimetallic MoFe/TiO2 nanospheres of highly efficacy in solar-light-driven peroxymonosulfate activation for organic pollutants removal. Applied Catalysis B: Environmental, 2021, 286, 119930.	20.2	110
12	Encapsulating Cobalt into N-Doping Hollow Frameworks for Efficient Cascade Catalysis. Inorganic Chemistry, 2021, 60, 9757-9761.	4.0	10
13	Engineering Electronic Structure of Single-Atom Pd Site on Ti 0.87 O 2 Nanosheet via Charge Transfer Enables C–Br Cleavage for Room-Temperature Suzuki Coupling. CCS Chemistry, 2021, 3, 1453-1462.	7.8	12
14	Stable Radicals with Protective Umbrellas Integrated on the Surface of 2D Layered Materials. Advanced Functional Materials, 2021, 31, 2104246.	14.9	2
15	Shape-dependent catalytic properties of electrochemically synthesized PdPt nanoparticles towards alcohols electrooxidation. Journal of Electroanalytical Chemistry, 2021, 896, 115189.	3.8	6
16	Ru nanoparticles supported on partially reduced TiO2 as highly efficient catalyst for hydrogen evolution. Nano Energy, 2021, 88, 106211.	16.0	43
17	Titanium nitride nanocrystals anchored evenly on interconnected carbon nanosheets with effective chemisorption and catalytic effects towards polysulfides for long-life lithiumâ^'sulfur batteries. Electrochimica Acta, 2021, 395, 139208.	5.2	6
18	High-index faceted Pt-Ru alloy concave nanocubes with enhancing ethanol and CO electro-oxidation. Electrochimica Acta, 2021, 396, 139266.	5.2	8

#	Article	IF	CITATIONS
19	Efficient electrocatalytic water splitting by bimetallic cobalt iron boride nanoparticles with controlled electronic structure. Journal of Colloid and Interface Science, 2021, 604, 650-659.	9.4	32
20	Nano-Ni-MOFs: High Active Catalysts on the Cascade Hydrogenation of Quinolines. Catalysis Letters, 2021, 151, 2445-2451.	2.6	8
21	Design of Binary Cu–Fe Sites Coordinated with Nitrogen Dispersed in the Porous Carbon for Synergistic CO <sub>2</sub> Electroreduction. Small, 2021, 17, e2006951.	10.0	63
22	Transformation of the sp <sup>2</sup> Carbanion to Carbene with Subsequent 1,1-Migratory Insertion and Nucleophilic Substitution in Rare-Earth Metal Chemistry. Inorganic Chemistry, 2021, 60, 18843-18853.	4.0	4
23	Enhancing electrocatalytic nitrogen reduction to ammonia with rare earths (La, Y, and Sc) on high-index faceted platinum alloy concave nanocubes. Journal of Materials Chemistry A, 2021, 9, 26277-26285.	10.3	20
24	Insights into the Pt/Rh(1â€ <sup>-</sup> 1â€ <sup>-</sup> 1) interface for direct ethanol fuel cells. Applied Surface Science, 2020, 502, 144093.	6.1	9
25	Synergetic Effect of Ru and NiO in the Electrocatalytic Decomposition of Li <sub>2</sub> CO <sub>3</sub> to Enhance the Performance of a Li-CO <sub>2</sub> /O <sub>2</sub> Battery. ACS Catalysis, 2020, 10, 1640-1651.	11.2	85
26	An Fe-doped Co11(HPO3)8(OH)6 nanosheets array for high-performance water electrolysis. Electrochimica Acta, 2020, 334, 135616.	5.2	13
27	Hydrazine Oxidation Reaction: Porous Carbon Membraneâ€Supported Atomically Dispersed Pyrroleâ€Type FeN <sub>4</sub> as Active Sites for Electrochemical Hydrazine Oxidation Reaction (Small 31/2020). Small, 2020, 16, 2070171.	10.0	2
28	Insights into ethanol electro-oxidation over solvated Pt(1 0 0): Origin of selectivity and kinetics revealed by DFT. Applied Surface Science, 2020, 533, 147505.	6.1	10
29	Dehydrogenative Coupling of Terminal Alkynes with O/N-Based Monohydrosilanes Catalyzed by Rare-Earth Metal Complexes. Inorganic Chemistry, 2020, 59, 14152-14161.	4.0	11
30	Electrochemically shape-controlled synthesis of great stellated dodecahedral Au nanocrystals with high-index facets for nitrogen reduction to ammonia. Chemical Communications, 2020, 56, 12162-12165.	4.1	15
31	Regulating the Hidden Solvationâ€Ionâ€Exchange in Concentrated Electrolytes for Stable and Safe Lithium Metal Batteries. Advanced Energy Materials, 2020, 10, 2000901.	19.5	65
32	PtCo@NCs with Short Heteroatom Active Site Distance for Enhanced Catalytic Properties. Advanced Functional Materials, 2020, 30, 2002281.	14.9	74
33	Porous Carbon Membraneâ€Supported Atomically Dispersed Pyrroleâ€Type FeN <sub>4</sub> as Active Sites for Electrochemical Hydrazine Oxidation Reaction. Small, 2020, 16, e2002203.	10.0	34
34	Fe Single Atoms and Fe <sub>2</sub> O <sub>3</sub> Clusters Liberated from N-Doped Polyhedral Carbon for Chemoselective Hydrogenation under Mild Conditions. ACS Applied Materials & Interfaces, 2020, 12, 34122-34129.	8.0	47
35	Suppressing lithium dendrite growth by a synergetic effect of uniform nucleation and inhibition. Journal of Materials Chemistry A, 2020, 8, 4300-4307.	10.3	29
36	Excavated cubic platinum–iridium alloy nanocrystals with high-index facets as highly efficient electrocatalysts in N <sub>2</sub> fixation to NH <sub>3</sub> . Chemical Communications, 2019, 55, 9335-9338.	4.1	48

#	Article	IF	CITATIONS
37	Fe/Fe <sub>3</sub> C Encapsulated in N-Doped Carbon Tubes: A Recyclable Catalyst for Hydrogenation with High Selectivity. Inorganic Chemistry, 2019, 58, 9469-9475.	4.0	40
38	Concave Cubic Pt–Sm Alloy Nanocrystals with High-Index Facets and Enhanced Electrocatalytic Ethanol Oxidation. ACS Applied Energy Materials, 2019, 2, 7204-7210.	5.1	19
39	High Catalytic Activity of Pt(100) for CH <sub>4</sub> Electrochemical Conversion. ACS Catalysis, 2019, 9, 10159-10165.	11.2	13
40	Does the oxophilic effect serve the same role for hydrogen evolution/oxidation reaction in alkaline media?. Nano Energy, 2019, 62, 601-609.	16.0	68
41	Visualization of facet-dependent pseudo-photocatalytic behavior of TiO2 nanorods for water splitting using In situ liquid cell TEM. Nano Energy, 2019, 62, 507-512.	16.0	44
42	Pd Nanocrystals with Continuously Tunable High-Index Facets as a Model Nanocatalyst. ACS Catalysis, 2019, 9, 3144-3152.	11.2	68
43	Clarifying the controversial catalytic active sites of Co <sub>3</sub> O <sub>4</sub> for the oxygen evolution reaction. Journal of Materials Chemistry A, 2019, 7, 23191-23198.	10.3	115
44	Regulating locations of active sites: a novel strategy to greatly improve the stability of PtAu electrocatalysts. Chemical Communications, 2019, 55, 13602-13605.	4.1	8
45	Core–Shell Structured S@Co(OH) <sub>2</sub> with a Carbon-Nanofiber Interlayer: A Conductive Cathode with Suppressed Shuttling Effect for High-Performance Lithium–Sulfur Batteries. ACS Applied Materials & Interfaces, 2019, 11, 4065-4073.	8.0	35
46	Longâ€Life Roomâ€Temperature Sodium–Sulfur Batteries by Virtue of Transitionâ€Metalâ€Nanocluster–Sul Interactions. Angewandte Chemie, 2019, 131, 1498-1502.	fur 2.0	63
47	Longâ€Life Roomâ€Temperature Sodium–Sulfur Batteries by Virtue of Transitionâ€Metalâ€Nanocluster–Sul Interactions. Angewandte Chemie - International Edition, 2019, 58, 1484-1488.	fur <sub>13.8</sub>	165
48	Ordered platinum–bismuth intermetallic clusters with Pt-skin for a highly efficient electrochemical ethanol oxidation reaction. Journal of Materials Chemistry A, 2019, 7, 5214-5220.	10.3	48
49	Cu <sup>2+</sup> Dual-Doped Layer-Tunnel Hybrid Na <sub>0.6</sub> Mn <sub>1–<i>x</i></sub> Cu <sub><i>x</i></sub> O <sub>2</sub> as a Cathode of Sodium-Ion Battery with Enhanced Structure Stability, Electrochemical Property, and Air Stability. ACS Applied Materials &: Interfaces. 2018. 10. 10147-10156.	8.0	98
50	Identifying the key obstacle in photocatalytic oxygen evolution on rutile TiO2. Nature Catalysis, 2018, 1, 291-299.	34.4	212
51	Novel Sulfur Host Composed of Cobalt and Porous Graphitic Carbon Derived from MOFs for the High-Performance Li–S Battery. ACS Applied Materials & Interfaces, 2018, 10, 13499-13508.	8.0	54
52	Ammonia electrooxidation on dendritic Pt nanostructures in alkaline solutions investigated by in-situ FTIR spectroscopy and online electrochemical mass spectroscopy. Journal of Electroanalytical Chemistry, 2018, 819, 495-501.	3.8	34
53	Effects of atom arrangement and thickness of Pt atomic layers on Pd nanocrystals for electrocatalysis. Electrochimica Acta, 2018, 271, 519-525.	5.2	6
54	Modelling the aqueous and nonaqueous interfaces for CO2 electro-reduction over Sn catalysts. Applied Surface Science, 2018, 428, 514-519.	6.1	3

#	Article	IF	CITATIONS
55	Constructing canopy-shaped molecular architectures to create local Pt surface sites with high tolerance to H <sub>2</sub> S and CO for hydrogen electrooxidation. Energy and Environmental Science, 2018, 11, 166-171.	30.8	32
56	Electrostatic Self-Assembly Enabling Integrated Bulk and Interfacial Sodium Storage in 3D Titania-Graphene Hybrid. Nano Letters, 2018, 18, 336-346.	9.1	40
57	Atomic cobalt as an efficient electrocatalyst in sulfur cathodes for superior room-temperature sodium-sulfur batteries. Nature Communications, 2018, 9, 4082.	12.8	305
58	Nickel Complexes with Nonâ€innocent Ligands as Highly Active Electrocatalysts for Hydrogen Evolution. Chinese Journal of Chemistry, 2018, 36, 1161-1164.	4.9	10
59	Edge-Site Engineering of Atomically Dispersed Fe–N <sub>4</sub> by Selective C–N Bond Cleavage for Enhanced Oxygen Reduction Reaction Activities. Journal of the American Chemical Society, 2018, 140, 11594-11598.	13.7	603
60	Unexpected effects of zirconium-doping in the high performance sodium manganese-based layer-tunnel cathode. Journal of Materials Chemistry A, 2018, 6, 13934-13942.	10.3	32
61	Novel 3.9 V Layered Na <sub>3</sub> V <sub>3</sub> (PO <sub>4</sub> ) <sub>4</sub> Cathode Material for Sodium Ion Batteries. ACS Applied Energy Materials, 2018, 1, 3603-3606.	5.1	23
62	Insights into the Distinct Lithiation/Sodiation of Porous Cobalt Oxide by in Operando Synchrotron X-ray Techniques and Ab Initio Molecular Dynamics Simulations. Nano Letters, 2017, 17, 953-962.	9.1	30
63	Electrochemical reduction of CO <sub>2</sub> into CO on Cu(100): a new insight into the C–O bond breaking mechanism. Chemical Communications, 2017, 53, 2594-2597.	4.1	39
64	Shape transformation of {hk0}-faceted Pt nanocrystals from a tetrahexahedron into a truncated ditetragonal prism. Chemical Communications, 2017, 53, 3236-3238.	4.1	17
65	An insight into methanol oxidation mechanisms on RuO <sub>2</sub> (100) under an aqueous environment by DFT calculations. Physical Chemistry Chemical Physics, 2017, 19, 7476-7480.	2.8	15
66	Constructing a Triple-Phase Interface in Micropores to Boost Performance of Fe/N/C Catalysts for Direct Methanol Fuel Cells. ACS Energy Letters, 2017, 2, 645-650.	17.4	89
67	Nanocrystal Catalysts of High-Energy Surface and Activity. Studies in Surface Science and Catalysis, 2017, 177, 439-475.	1.5	2
68	Dodecahedral W@WC Composite as Efficient Catalyst for Hydrogen Evolution and Nitrobenzene Reduction Reactions. ACS Applied Materials & Interfaces, 2017, 9, 20594-20602.	8.0	28
69	Identifying the significance of proton-electron transfer in CH4 production on Cu (100) in CO2 electro-reduction. Journal of Electroanalytical Chemistry, 2017, 793, 184-187.	3.8	10
70	Platinum–Cobalt Bimetallic Nanoparticles with Pt Skin for Electro-Oxidation of Ethanol. ACS Catalysis, 2017, 7, 892-895.	11.2	89
71	Graphitized porous carbon materials with high sulfur loading for lithium-sulfur batteries. Nano Energy, 2017, 32, 503-510.	16.0	118
72	Octahedral PtCu alloy nanocrystals with high performance for oxygen reduction reaction and their enhanced stability by trace Au. Nano Energy, 2017, 33, 65-71.	16.0	139

#	Article	IF	CITATIONS
73	Urea hydrogen bond donor-mediated synthesis of high-index faceted platinum concave nanocubes grown on multi-walled carbon nanotubes and their enhanced electrocatalytic activity. Physical Chemistry Chemical Physics, 2017, 19, 31553-31559.	2.8	16
74	Free energy landscape of electrocatalytic CO 2 reduction to CO on aqueous FeN 4 center embedded graphene studied by ab initio molecular dynamics simulations. Chemical Physics Letters, 2017, 688, 37-42.	2.6	20
75	Designing Pt-Based Electrocatalysts with High Surface Energy. ACS Energy Letters, 2017, 2, 1892-1900.	17.4	46
76	Cu overlayers on tetrahexahedral Pd nanocrystals with high-index facets for CO <sub>2</sub> electroreduction to alcohols. Chemical Communications, 2017, 53, 8085-8088.	4.1	64
77	Seeds and Potentials Mediated Synthesis of High-Index Faceted Gold Nanocrystals with Enhanced Electrocatalytic Activities. Langmuir, 2017, 33, 6991-6998.	3.5	30
78	Electrochemical interfacial influences on deoxygenation and hydrogenation reactions in CO reduction on a Cu(100) surface. Physical Chemistry Chemical Physics, 2016, 18, 15304-15311.	2.8	6
79	Insights into the mechanism of nitrobenzene reduction to aniline over Pt catalyst and the significance of the adsorption of phenyl group on kinetics. Chemical Engineering Journal, 2016, 293, 337-344.	12.7	96
80	Elucidation of the surface structure–selectivity relationship in ethanol electro-oxidation over platinum by density functional theory. Physical Chemistry Chemical Physics, 2016, 18, 15501-15504.	2.8	20
81	Hydrogen adsorption-mediated synthesis of concave Pt nanocubes and their enhanced electrocatalytic activity. Nanoscale, 2016, 8, 11559-11564.	5.6	39
82	Structure Design and Performance Tuning of Nanomaterials for Electrochemical Energy Conversion and Storage. Accounts of Chemical Research, 2016, 49, 2569-2577.	15.6	131
83	Insight into the promoting role of Rh doped on Pt(111) in methanol electro-oxidation. Journal of Electroanalytical Chemistry, 2016, 781, 24-29.	3.8	19
84	In-situ FTIR spectroscopic studies of electrocatalytic reactions and processes. Nano Energy, 2016, 29, 414-427.	16.0	108
85	Insight into CO Activation over Cu(100) under Electrochemical Conditions. Electrochimica Acta, 2016, 190, 446-454.	5.2	19
86	Methanol electro-oxidation on platinum modified tungsten carbides in direct methanol fuel cells: a DFT study. Physical Chemistry Chemical Physics, 2015, 17, 25235-25243.	2.8	46
87	The origin of high activity but low CO2 selectivity on binary PtSn in the direct ethanol fuel cell. Physical Chemistry Chemical Physics, 2014, 16, 9432-9440.	2.8	56
88	Significance of β-dehydrogenation in ethanol electro-oxidation on platinum doped with Ru, Rh, Pd, Os and Ir. Physical Chemistry Chemical Physics, 2014, 16, 13248-13254.	2.8	44
89	Role of Water and Adsorbed Hydroxyls on Ethanol Electrochemistry on Pd: New Mechanism, Active Centers, and Energetics for Direct Ethanol Fuel Cell Running in Alkaline Medium. Journal of Physical Chemistry C, 2014, 118, 5762-5772.	3.1	73
90	Engineering Electronic Structure of Single-Atom Pd Site on Ti 0.87 O 2 Nanosheet via Charge Transfer Enables C-Br Cleavage for Room Temperature Suzuki Coupling. CCS Chemistry, 0, , 1-29.	7.8	0